Fatigue characterization of asphalt concrete using Schapery´s Work Potential Model

Robert Lundström and Jonas Ekblad

Royal Institute of Technology, Division of Highway Engineering
SE-100 44, Stockholm, Sweden.
robert.lundstrom@ncc.se, ekblad@byv.kth.se

ABSTRACT

This paper presents an investigation of Schapery´s work potential theory (WPT), a constitutive viscoelastic continuum damage model, applied to characterize fatigue behavior of asphalt concrete. Although some anomalies were noted, results indicate that the model is applicable to characterize fatigue-related damage growth at different loading modes, excitation amplitudes and temperatures.

INTRODUCTION

Fatigue-related cracking is a major distress mechanism of highly trafficated asphalt pavements. The ability of a given asphalt mixture to resist crack initiation and propagation is largely governed by mixture composition and rheology.

During the years, several different approaches have been employed to characterize fatigue deterioration, approaches which may be classified as classical, fracture and damage mechanics.

Damage mechanics models are usually formulated within the general frameworks of continuum mechanics and thermodynamics and focuses on the description of constitutive material behavior as influenced by microcracking in contrast to fracture mechanics where deterioration is characterized by macro-crack growth. Consequently, damage mechanics models often ignore the physical details of defects and instead records macroscopic response (e.g. stiffness).

Schapery has developed a group of damage mechanics models which accentuate intrinsic viscoelasticity[1, 2, 3, 4, 5, 6, 7], among some is based on the so-called Work Potential Theory (WPT).

The purpose of this paper is to investigate the applicability of the viscoelastic continuum damage model based on the work potential theory (WPT) to characterize fatigue deterioration in asphalt mixtures.

THEORY

In principle, the WPT damage model is based on two parts: linear viscoelastic characterization and nonlinear damage accumulating, respectively.

Linear viscoelasticity

Linear viscoelastic behavior is a special type of time-dependent constitutive behavior, which is characterized by the general principle that effects of sequential changes in input (stress or strain) are additive.

Uniaxial linear viscoelastic behavior is generally expressed as either complex modulus, $E^*(\omega)$, relaxation modulus, $E(t)$, or creep compliance, $D(t)$. The norm of complex modulus, often called dynamic modulus, represents stiffness at sinusoidal excitation and is defined as the ratio between the amplitudes of stress and strain signals, while the phase angle represents the time-dependence.

Generally, viscoelastic materials, such as asphalt concrete, exhibit in addition to time (or frequency) dependence significant tem-

perature dependence. By the so-called time-temperature superposition principle, construction of composite master curves from horizontally shifted isotherms is possible for so-called thermorheologically simple materials[8]. Consequently, the dependence of material properties as $E(t,T)$ upon time and temperature can be represented solely by a single parameter, reduced time, ξ:

$$\xi = \int_0^t \frac{dt'}{a_T(T(t'))} \qquad (1)$$

where t' is time and a_T is a temperature dependent function, which reflects the influence of temperature on mechanical behavior under transient temperature.

Nonlinear viscoelasticity

At sufficiently high excitation levels, asphalt mixtures exhibit nonlinear behavior, which may be modeled as either intrinsic stress dependent (e.g. Shields et al[9]) or as a consequence of distributed damage (e.g. Kim et al[10]). In the latter case, the nonlinearity can be treated within the framework of damage mechanics, as it is regarded as an irreversible phenomenon. This in turn means that the damage is fully characterized by changes in damage parameters, and the resulting mechanical response is a function of these parameters. Using the WPT model the existence of a pseudostrain energy function, W^R, which is a function of so-called pseudostrain, ε^R, and a single damage parameter denoted S_1 is postulated.

$$W^R \equiv W^R(\varepsilon^R, S_1) \qquad (2)$$

For the purpose of this paper, the definition of uniaxial pseudostrain, ε^R, for isothermal conditions materials proceeds from a single linear relaxation function:

$$\varepsilon^R(t) \equiv \frac{1}{E_R}\int_0^t E(t-\tau)\frac{d\varepsilon}{d\tau}d\tau \qquad (3)$$

where E_R is the so-called reference modulus (usually set equal to one), which is an arbitrary constant having the same unit as the relaxation modulus $E(t)$. ε is actual strain.

Under the assumption of steady-state sinusoidal loading, pseudo strain can be approximated as:

$$\varepsilon^R = \frac{1}{E_R}\left[\varepsilon_0 |E^*| \sin(\varpi t + \phi + \theta)\right] \qquad (4)$$

where $|E^*|$ is dynamic modulus, ϖ frequency, ϕ phase angle and θ a constant

The constitutive model is obtained by assuming Equation 2 to take the form of a quadratic function of pseudostrain and letting the response be of Green type, i.e:

$$\sigma \equiv \frac{\partial W^R}{\partial \varepsilon^R} = C_1(S_1)\varepsilon^R \qquad (5)$$

By introducing the parameter pseudostiffness, $C_1(S_1)$, and the pseudostrain, ε^R, viscoelastic material behavior can in principle be described in the same way as elastic materials (elastic-viscoelastic correspondence), which is indicated in the functional form of Equation 5. Pseudostiffness, $C_1(S_1)$, represents a constitutive parameter, which explicitly depends on the non-physical damage parameter, S_1. In the case of growing damage, S_1 increases monotonically from zero and $C_1(S_1)$ decreases from one towards zero. From the definition of ε^R (Equation 4), it can be observed that pseudostrain simply is the predicted dimensionless stress response occurring during negligible damage. Hence, any deviation in output (stress or strain) from the theoretical value is reflected by Equation 5. Consequently, stress-pseudostrain relationships provide a correspondence between linear viscoelastic undamaged and damaged bodies.

Any time-dependent damage growth is accounted for using Equation 4, which describes the evolution of the single structural parameter, S_1.

$$\dot{S}_1 \equiv \left(-\frac{\partial W^R}{\partial S_1}\right)^{\alpha_1} \qquad (6)$$

where α_1 is a material constant, related to the inherent time-dependence of the material. Even though α_1 is denoted material constant, its value may depend on fracture characteristics of the material. The value of α_1 for asphalt mixtures has been approximated by Equation 7[11].

$$\alpha_1 \equiv 1 + \frac{1}{m} \qquad (7)$$

where m is the maximum slope of the relaxation modulus on log-log scale.

In Park (1994)[12] and Park & Schapery (1997)[13] it was shown that it might be possible to describe and predict damage growth in solid propellant, a viscoelastic composite material resembling of asphalt concrete, at different temperatures and loading rates, if physical time is replaced by reduced time. The ability to predict damage growth at different temperatures may be possible if reduced time is used in pseudostrain (Equation 3) as well as the in damage evolution law (Equation 6).

EXPERIMENTAL

Materials

The six asphalt mixtures tested in the current investigation consisted of dense-graded asphalt concrete with one and the same aggregate size distribution with maximum aggregate size 11 mm. Three conventional base bitumens, penetration grades 50/60, 70/100 and 160/220 (Laguna, Venezuela) and three polymer modified bitumens, where used. Modification was achieved by adding Styrene-Butadiene-Styrene (SBS) to the base bitumens mentioned above at 5 and 10 % by weight. The modified mixes are denoted M and amount of modifier, e.g. 70/100M5 corresponds to SBS modified base bitumen 70/100 with 5 % additive. The target binder and air void content was chosen for all six materials studied to 6.2 % by weight and 3.4 % by volume, respectively.

The mixtures were compacted to slabs, using a laboratory rolling wheel compactor.

The slabs were sawn in halves, and cylinders with a diameter of 80 mm and length 120 mm were cored horizontally from each half.

Testing

The specimens described above were investigated by complex modulus and cyclic fatigue testing; all performed using unconfined uniaxial mode.
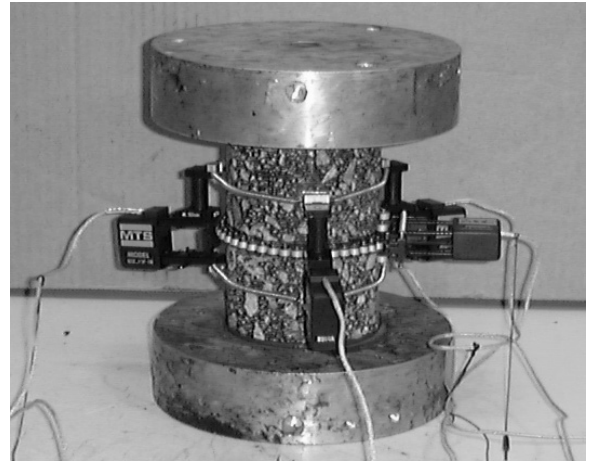

Figure 1. Test set-up for complex modulus and fatigue testing.

Axial deformations were measured using three on-sample strain-gauge extensometers, spaced 120° apart (cf. Figure 1).

During complex modulus testing, the specimens were subjected to a sinusoidally oscillating axial load in both tension and compression at constant strain amplitude ($50 \cdot 10^{-6}$ m/m). All tests were performed at five temperatures (-10, 0, 10, 20 and 30 °C) using nine frequencies (40, 32, 16, 8, 4, 2, 1, 0.5 and 0.1 Hz).

During cyclic fatigue testing, each specimen was subjected to a sinusoidally oscillating axial excitation in both tension and compression. The testing was performed using controlled stress or strain mode at a single frequency of 10 Hz at three temperatures 0, 10 or 20 °C. During the fatigue tests, the increase in sample temperature was recorded on the mid-height envelope surface of each specimen using a thermocouple.

RESULTS AND ANALYSIS

In short, the analysis procedure comprised two steps: complex modulus was interconverted to relaxation modulus, parameterized using Prony-series, whereafter cyclic (fatigue) tests were analyzed using the WPT model and methodology mainly based on work done by Daniel & Kim[11].

Linear viscoelastic characteristics

Complex modulus testing provides dynamic modulus and phase angle data for each of the mixtures studied. In general, comparatively high consistency was observed at most frequencies within the temperature range studied (-10 to +30 °C) as indicated by elliptic hysteresis loops as well as by high frequency contents as determined by Fast Fourier Transform analysis.

The complex modulus data were used to construct dynamic modulus and phase angle master curves, subsequentially interconverted to relaxation modulus using the method described by Schapery and Park[14].

A comparison of master relaxation modulus curves of the 160/220, 160/220M5 and 160/220M10 is shown in Figure 2. As illustrated, at sufficiently long relaxation time the effect of polymer modification is obvious as the two modified mixtures show higher relaxation modulus at a given reduced time.
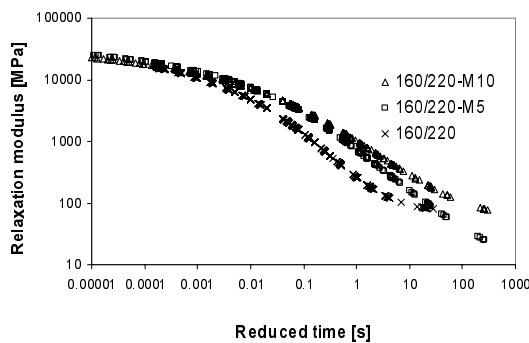

Figure 2. Relaxation modulus of base and modified mixes at 10 °C.

In order to analytically represent the relaxation modulus, $E(\xi)$, Prony series generally containing 10 Maxwell elements were fitted according to:

$$E(\xi) = E_\infty + \sum_{i=0}^{M} E_i \cdot e^{-\frac{\xi}{\rho_i}} \qquad (8)$$

Cyclic fatigue tests

The fatigue testing in this study covered an overall range in initial stiffness between 1800 and 21000 MPa depending on material and test temperature used. Figure 3 illustrates five controlled strain fatigue tests carried out at 10 °C using the 160/220M5 mixture.
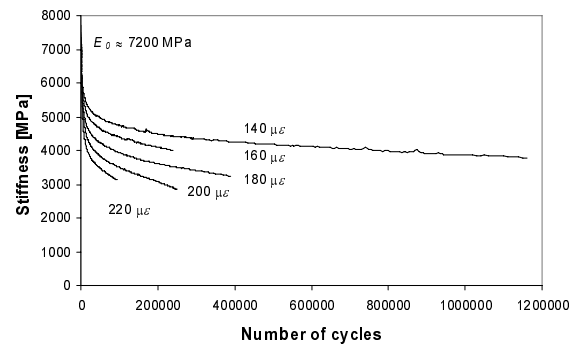

Figure 3. Fatigue paths of strain controlled tests (160/220M5 mixture at 10 °C).

Damage evolution was modeled using Equations 1-7, where the initial loading ramp is treated using a piece-wise linear approximation and the subsequent cyclic loadings are evaluated using the steady-state assumption[11]. At cyclic loading, it is assumed that only one-fourth of the total loading cycle (the positive tensile part) is responsible for the damage growth[11].

The results shown in Figure 4 indicate that the entire deterioration process can be reasonable well described by using practically a single characteristic curve. However, it was observed that some low amplitude tests (high cycle fatigue tests) significantly deviates from the common path, and consequently, does not follow the same curve as the other tests. It should be mentioned that all curves presented in Figure 4 were obtained using the same definition of the α_1

(cf. Equation 7). It could be argued that a change in the α_1-value may provide a better collapse of the curves shown in Figure 4. However, such a procedure is doubtful as it implies that α_1 simply is a fitting parameter and not based on a theoretical model.
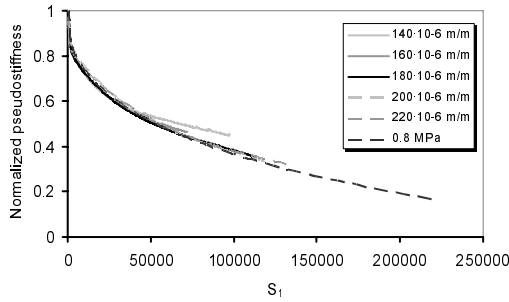

Figure 4. $C_1(S_1)$ curves obtained from controlled strain and controlled stress tests (160/220M5 mixture at 10 °C).

The results shown in Figure 4 are representative for most materials and conditions used in this study at controlled strain testing but also controlled stress testing.

As also indicated in Figure 4, there may be relatively large differences between different samples regarding decrease in pseudostiffness at failure. The comparably large differences are partly explained by the stochastic process leading to failure due to sample-to-sample variability, as illustrated in Figure 3 and discussed by Lundström et al[15]. From results presented hitherto on cyclic tests, it may be concluded, that the model seems to be suitable for describing the deterioration process during fatigue testing independent of stress or strain level as well as mode of loading at 10 °C for all mixtures studied.

It was also investigated whether it is possible to use the time-temperature superposition principle to obtain a material function, $C_1(S_1)$, independent of temperature. In Figure 5, damage curves obtained at 0 and 20 °C are shifted to the reference temperature 10 °C using reduced time instead of real time when calculating damage evolution. The results indicate that it is possible to

model deterioration at different temperatures, except at too soft conditions. For example, for the softest mixture used (160/220) at 20 °C it was not possible to obtain a $C_1(S_1)$ path close to those obtained at 0 and 10 °C. The resulting accuracy for predicting deterioration path (stiffness vs. number of cycles) was regarded as satisfying compared to predictions based on the temperature specific curves. However, the main difficulty in predicting fatigue life of a given test concerns prediction of failure during controlled strain testing. Even though the shape of the fatigue path is relatively accurately predicted, total fatigue life largely depends on level of stiffness at failure, which is much more difficult to predict.
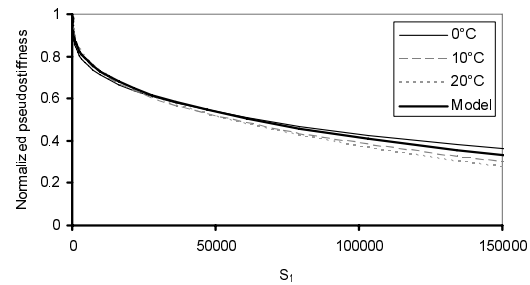

Figure 5. Temperature specific curves obtained at 0, 10 and 20 °C and the corresponding model curve (160/220M10 mixture, reference temperature 10 °C).

The cyclic test results presented above were obtained under the assumption of constant temperature during testing. However, such an assumption has been questioned in several papers[16,17]. When asphalt concrete samples are cyclically loaded, energy dissipation results in heat generation, which in turn influences temperature. To get information about the magnitude of the hysteretic heating, the increase in temperature was recorded on the envelope surface of each sample using thermocouples. The temperature recorded during controlled strain tests reached a maximum at approximately 10,000 to 50,000 cycles for all mixtures and temperatures used, as illustrated in Figure 6. In general, tests carried out at 0 °C led to

comparably small increase in temperature, while tests at 10 and 20 °C could lead to moderate or relatively high increase in temperature. Depending on test conditions, an increase in temperature up to 3 °C at failure was recorded.
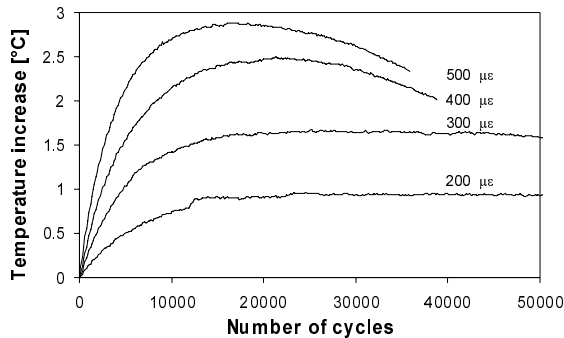

Figure 6. Temperature increase during controlled strain fatigue tests (70/100M5, 20 °C).

The increase in temperature may significantly influence the stiffness, depending on the thermal susceptibility of the mixture. Figure 7 shows the dependence of dynamic modulus of the 70/100M5 mixture on temperature as well as relative decrease due to change in temperature.
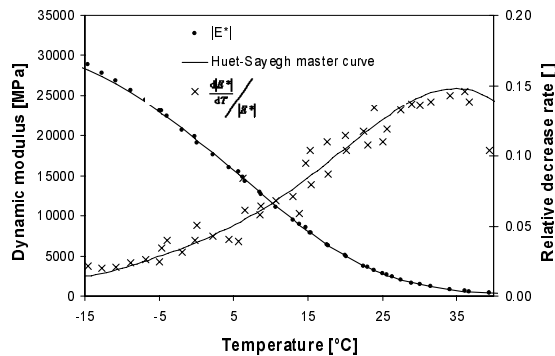

Figure 7. Dynamic modulus and relative decrease as function of temperature (70/100M5 at 10 Hz).

The figure indicates that an increase in temperature of one degree C results in a decrease in stiffness of approximately 4, 7 and 12 percent at 0, 10 and 20 °C, respectively. Furthermore, results presented indi-cate that the influence of hysteric heating at cyclic tests may be pronounced, especially at higher temperature. If the fatigue test is performed at 20 °C and a temperature increase in one °C means 12 percent decrease in dynamic stiffness, an increase in temperature of 3 °C during fatigue testing undoubtedly influences test results.

To visualize this phenomenon, temperature adjusted damage evolution curve for the 70/100M5 mixture at 10 °C is compared to the originally calculated uncorrected curve (Figure 8). The adjustment was achieved by using reduced time, estimated from the transient temperature and corresponding shift factor (a_T) in the damage evolution.
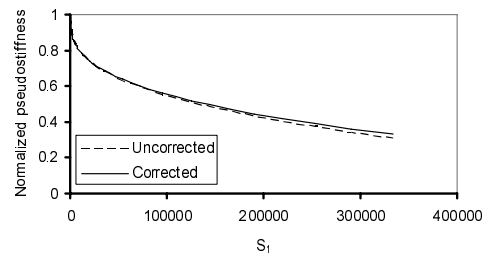

Figure 8. $C_1(S_1)$ curves obtained from cyclic tests using uncorrected and corrected temperature data (70/100M5 at 10 °C).

Visually, from Figure 8, the difference between adjusted and unadjusted curves seems only very small. However, even fairly large differences in test results often gives visually similar results when expressed as $C_1(S_1)$. In Figure 9, predictions of controlled strain tests using the adjusted (Corrected) and unadjusted (Experimental) curves respectively, expressed as stiffness decrease by number of cycles, are shown.

Assuming fracture defined as 50 % reduction in stiffness the fatigue life, indicated by arrows, differs by approximately 40 %. It could be argued that this difference is of a magnitude comparable to repeatability thus of minor importance. However, it should be noted that the difference is systematic.
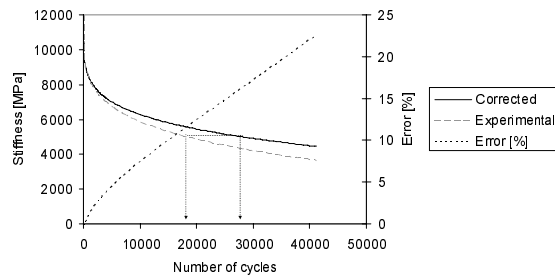
Figure 9. Simulations of $200 \cdot 10^{-6}$ m/m controlled strain test based on corrected and uncorrected characteristic curves, respectively (70/100M5 at 10 °C).

DISCUSSION

Cyclic fatigue at different excitation levels and modes (strain or stress controlled) were, in general, successfully modeled using the model described. Nevertheless, for very soft materials or tests that required a large number of cycles to fracture, some anomalies were noted. Cyclic tests performed relatively close to a fatigue threshold value, that is, a loading level not high enough to cause as significant damage growth as shown at higher excitation amplitudes, deviates from tests with a higher rate of damage accumulation. Accordingly, different mechanisms may be present during different testing modes. It is well known from fracture mechanics that near-threshold fatigue characterization using Paris´ law is difficult[18]. Close to the so-called fatigue threshold, cracks either remain dormant or grow at undetectable rates. A similar phenomenon may occur during cyclic testing of asphalt concrete. Furthermore, the model does not take into account beneficial processes as healing, which may be present even during cyclic loading[19]. Consequently, comparably long fatigue tests may be exposed to more beneficial processes compared to short tests.

Since the model largely is phenomenological, the specific nature of different mechanisms acting during destructive testing may not be easily characterized and distinguished from each other. However, even though several questions still are to be an-

swered, the model based on the WPT remains interesting, and is possibly, the most versatile damage model for asphalt characterization available today.

CONCLUSIONS

Based on the results presented the following conclusions can be drawn:

- Although, some anomalies were noted, the results indicate that the WPT is applicable to characterize fatigue-related damage growth in asphalt concrete mixtures at different loading modes, excitation amplitudes and temperatures.
- The results also indicate a pronounced effect of polymer modification on linear viscoelastic and fatigue characteristics. In general, SBS modification increases fatigue life, both in terms of stiffness-decrease rate and critical level of damage at failure.
- Increase in sample temperature due to hysteretic heating influences the stiffness, and should consequently, be taken into account.

ACKNOWLEDGEMENT

REFERENCES

1. Schapery, R. A. (1981),"On Viscoelastic Deformation and Failure Behaviour of Composite Materials with Distributed Flaws", Advances in Aerospace Structures and Materials (eds. Wang & Renton), ASME, **1**, 5-20

2. Schapery, R. A. (1982), "Models for Damage Growth and Fracture in Nonlinear Viscoelastic Particulate Composites", Pro-

ceedings Ninth U.S. National Congress of Applied Mechanics, ASME, 237-245.

3. Schapery R. A. (1984), "Correspondence Principles and a Generalized J-Integral for Large Deformation and Fracture Analysis of Viscoelastic Media", *Int. J. Fract.*, **25**, 195-223.

4. Schapery R. A. (1987), "Deformation and Fracture Characterization of Inelastic Composite Materials Using Potentials", *Polymer Engineering and Science*, **27**, 63-76.

5. Schapery R. A. (1990), "A Theory of Mechanical Behaviour of Elastic Media with Growing Damage and other changes in Structure", *J. Mech. Phys. Soc.*, **38**, 215-253.

6. Schapery, R. A. (1994), "Nonlinear Viscoelastic Constitutive Equations for Composite Materials based on Work Potentials", Proceedings 12th congress of applied mechanics (ed. Kobayashi), *Appl. Mech. Rev.*, **47**.

7. Schapery, R. A. (1999), "Nonlinear Viscoelastic and Viscoplastic Constitutive Equations with Growing Damage", *International Journal of Fracture*, **97**, 33-66.

8. Ferry, J. D. (1980), "Viscoelastic Properties of Polymers.", 3rd edition John Wiley & Sons.

9. Shields, D. H., Zeng, M., Kwok, R. (1998), "Nonlinear Viscoelastic Behaviour of Asphalt Concrete in Stress Relaxation" *The Association of Asphalt Paving Technologists*, **67**, 358-400.

10. Kim, Y. R., Lee, H. J., Little, D. N. (1997), "Fatigue Characterization of Asphalt Concrete Using Viscoelasticity and Continuum Damage Theory", *Journal of the Association of Asphalt Paving Technologists*, **66**, 520-569.

11. Daniel, J. S., Kim, Y. R. (2002), "Development of a Simplified Fatigue Test and Analysis Procedure Using a Viscoelastic, Continuum Damage Model", *Journal of the Association of Asphalt Paving Technologists*, **71**.

12. Park, S. W. (1994), "Development of a nonlinear thermoviscoelastic constitutive equation for particulate composites with growing damage", PhD dissertation, The University of Texas, Austin.

13. Park, S. W., Schapery, R. A. (1997), "A Viscoelastic Constitutive Model for Particulate Composites with Growing Damage", *Int. J. Solids Structures*, **34**, 931-947.

14. Schapery, R. A., Park, S. W. (1999), "Methods of interconversion between linear viscoelastic functions. Part II-an approximate analytical method", *International Journal of Solids and Structures*, **36**, 1677-1699.

15. Lundström, R., Di Benedetto, H., Isacsson, U. (2004), "Influence of asphalt mixture stiffness on fatigue failure", *Journal of Materials in Civil Engineering*, **16**, 516-525.

16. Di Benedetto, H., Soltani, A. A., Chaverot, P. (1996), "Fatigue Damage for Bituminous Mixtures: A Pertinent Approach", *Journal of the Association of Asphalt Paving Technologists*, **65**, 142-158.

17. Di Benedetto, H., De La Roche, C. (1998), "State of the Art on Stiffness Modulus and Fatigue of Bituminous Mixtures", Rilem Report 17, Bituminous Binders and Mixtures, ed. L Francken, E&FN Spon, London.

18. Chehab, G. R. Kim, Y. R., Schapery, R. A., Witczak, M. W., Bonaquist, R. (2003), "Characterization of Asphalt Concrete in Uniaxial Tension using a Viscoelasticplastic Model." *Proceedings of the Journal of the Association of Asphalt Paving Technologists* (AAPT), **72**, 315-355.

19. Pronk, A. C., Molenaar, J. M. M. (1997), "Harmonization of 2 and 4 Point Dynamic Bending Tests Based on a 'New' Fatigue Life Definition", Mechanical Tests for Bituminous Materials, Di Benedetto & Francken, eds.